Available online at www.sciencedirect.com

ScienceDirect

IFAC Papers Online CONFERENCE PAPER ARCHIVE

IFAC-PapersOnLine 49-26 (2016) 270–276

A Comparative Analysis of Dynamic Models of the Central Carbon Metabolism of *Escherichia coli*

Ana Patrícia Lima*. Vítor Baixinho.*Daniel Machado. Isabel Rocha ***

Centre of Biological Engineering
University of Minho, Campus de Gualtar
4710-057 Braga - Portugal

* *These authors have contributed equally to this work*

Abstract: Dynamic models of metabolism have been developed for a variety of systems and can be applied in metabolic engineering design and to understand the time-varying characteristics of the systems when exposed to different stimuli. Hereby we analyse and compare the most used and complete kinetic models available for the central carbon metabolism of *E. coli*. Stoichiometric and kinetic comparisons showed several differences, discrepancies and incoherence especially regarding the kinetic mechanisms assumed, parameters and units. Time course and steady-state simulations and also comparison with an experimental dataset put in evidence major differences regarding responses to the same stimulus. The results presented raise important questions regarding the need of using standard methodologies in dynamic model construction as well as in using experimental data for model validation.

Keywords: Kinetic Models; *Escherichia coli*; Time course simulation; Steady-State

1. INTRODUCTION

Mathematical models help understand, predict, and optimize the properties and behaviour of cell factories. For that reason, they assume a great importance in industrial biotechnology. In order to study cellular metabolism, there are two main different modelling approaches based on different assumptions: kinetic and stoichiometric modelling (Machado et al. 2012) .

Kinetic models describe the temporal behaviour of all biochemical species in a metabolic system. They specify the details of interactions at metabolite and enzyme levels, such as allosteric regulation, therefore assuming a crucial role to a more explicit study of metabolic responses to perturbations at time-scales before a steady state is reached **(**Shmulevich 2011**)**.

Over the years, several dynamic models have been developed for different metabolic systems. Here four important dynamic models of the central metabolism of *Escherichia coli* are analysed (Chassagnole et al. 2002; Peskov et al. 2012; Kadir et al. 2010; and Khodayari et al. 2014).

The Chassagnole model is the oldest one and only describes kinetic equations for the glycolysis and pentose phosphate pathways; however, it is still widely utilized (Theobald et al. 1997; Vaseghi et al. 1999; Rizzi et al. 1997; Chassagnole et al. 2002). Meanwhile, three recent models have been published, covering other metabolic pathways, such as the tricarboxylic acids (TCA) cycle. The main goal of the Kadir model was to simulate the time profiles of batch and continuous cultures (Kadir et al. 2010). The Peskov model describes some metabolic regulations of *E. coli* central carbon metabolism (Peskov et al. 2012). The Khodayari model is the largest detailed *E. coli* kinetic model, accounting for a total of 138 reactions (1474 elementary reactions) and 93 metabolites (830 complexes and metabolites). This model was parameterized, with multiple *omics* data, using the ensemble modelling method (Toya et al. 2007; Tran et al. 2008)**.**

Besides the different pathway coverage, these models have been constructed with different applications in mind and with different assumptions and levels of experimental validation. However, a comparison of the coverage and performance of these models under the same conditions has not been performed so far, limiting any critical comparison between them.

Constraint-based methods can be used to determine intracellular metabolic fluxes based on mass balances over intracellular metabolites and the assumption of a pseudo-steady state. Contrary to the kinetic models, these models do not require the determination of kinetic equations and associated kinetic parameters, even though they are important to understand the capabilities of the metabolic network and to perform structural analysis (Szallasi 2006; Kuepfer 2014). In this work the *i*AF1260 genome-scale stoichiometric model of *E. coli* K-12 MG1655 was used for structural comparison purposes. This model encompasses 1260 genes, 2077 reactions and 1039 metabolites (Feist et al. 2007).

2. METHODS

2. 1 Dynamic models and standardization

The kinetic models used were the ones introduced by (Chassagnole et al. 2002); (Peskov et al. 2012); (Kadir et al. 2010) and (Khodayari et al. 2014).

10.1016/j.ifacol.2016.12.137

To allow comparing model predictions, all models were set to the same experimental conditions and prepared for simulation of a glucose pulse, as described by Chassagnole et al., 2002 with a dilution rate of 0.1 h^{-1} and a glucose concentration in the feed of 110.96 mM. For that purpose, the initial concentration of extracellular glucose was set to 2 mM. Considering a biomass concentration of 8.7 gDW/L and a cellular density of 564 gDW/L one obtains a ratio of 65 L of extracellular volume per 1 L of biomass.

The Chassagnole model is available at the BioModels Database (BioModels ID: BIOMD0000000051) (Le Novère et al. 2006; Juty et al. 2015; Li et al. 2010) in the SBML format. For this model, the extracellular to intracellular volume ratio (65:1) had been implicitly incorporated in the stoichiometry of the Phosphotransferase System (PTS). To facilitate comparisons with other models and allow to easily change this parameter, the ratio was defined in the respective compartment volumes and the PTS stoichiometry was fixed. It should be emphasized that this change does not affect the model predictions.

The Kadir model was provided in MATLAB code by the authors. An SBML version was constructed using JWS Online (Olivier & Snoep 2004).

The Peskov model had been downloaded from JWS Online in SBML (but it is no longer available). An external compartment, with volume equal to 65 L, was added to the model. The extracellular glucose was redefined from a parameter to a metabolite and the Glc_{in} metabolite was removed accordingly.

The Khodayari model was downloaded in MATLAB from the author's web page, which can be accessed at http://www.maranasgroup.com/submission_models/escherichiaColiCoreMetabolism.htm (Research Goup of Costas D. Maranas. 2014). An SBML version was constructed using JWS Online (Olivier & Snoep 2004).

In all models, a common equation for the extracellular glucose kinetics (as defined in the Chassagnole model) was added:

$$V_{glcex} = Dil \times ([Glc]_{feed} - [Glc]_{ext}) \quad (1)$$

where V_{glcex} is the extracellular glucose exchange rate, *Dil* is the system dilution rate, $[Glc]_{feed}$ is the glucose concentration in the feed and $[Glc]_{ext}$ is the extracellular concentration of glucose.

2.2 Units conversion

To facilitate comparison, all models were standardized to the same units. The ones commonly used in genome-scale models were chosen for that purpose. Therefore, metabolite concentrations and reaction rates were changed from mM and mM/s to mmol/gDW and mmol/gDW/h, respectively. The parameters were also converted, while dimensionless parameters were kept unchanged. Some discrepancies regarding the kinetic parameters were found. In some cases, there were differences between the parameter values in the models and those reported in the original papers. In those cases, the values present in the SBML file prevailed since they more accurately replicated the published results.

2.3 Changes in kinetic laws

Changes in some kinetic equations were performed, due to discrepancies found during the units' conversion step. The most common case was the re-arrangement of Hill equations to make the Hill coefficient explicit for the dissociation constants (otherwise it would lead to inconsistent units). For instance, in the Chassagnole model, the parameter $K_{PTS,g6p}$, had to be re-calculated, as it had been defined incoherently (in the inhibition term it appears as $\frac{C_{g6p}^{n_{PTS,g6p}}}{K_{PTS,g6p}}$). It was recalculated as follows:

$$K'_{PTS,g6p} = \sqrt[n_{PTS,g6p}]{K_{PTS,g6p}} \quad (2)$$

The recalculated parameter was then re-introduced in the PTS kinetic equation with an explicit Hill coefficient (eq. 3).

$$r_{PTS} = \frac{r_{max} \times C_{gluc} \times \frac{C_{pep}}{C_{pyr}}}{\left(K_{PTS,a1} + K_{PTS,a2} \times \frac{C_{pep}}{C_{pyr}} + K_{PTS,a3} \times C_{gluc} + C_{gluc} \times \frac{C_{pep}}{C_{pyr}}\right) \times \left(1 + \frac{C_{g6p}^{n_{PTS,g6p}}}{\boldsymbol{Knew}^{n_{PTS,g6p}}}\right)} \quad (3)$$

A similar procedure was applied to both the DAHP synthase (DAHPS) and the pyruvate dehydrogenase (PDH) reactions. Table 1 shows the values of each recalculated parameter and the new values in both units used.

Table 1 – Results for the re-estimation of some parameters for the Chassagnole model.

Parameter	Original value (mM)	New value	
		mM	mmol/gDW
$K_{PTS,g6p}$	2.15	1.23	0.0022
$K_{DAHPS,e4p}$	0.035	0.275	0.00049
$K_{DAHPS,pep}$	0.0053	0.0924	0.0002
$K_{PDH,pyr}$	1159	6.802	0.012

In the Kadir model, the kinetic equations for the PTS, aldolase (ALDO) and acetate kinase (ACK) reactions were also modified. The PTS kinetics is equal to the one described in the Chassagnole model and thus the changes were performed in the same way. The kinetic equations for ALDO and ACK had differences between the SBML and the ones reported in original article. The formulations present in the article were chosen since this option was the only one that allowed obtaining an agreement in the validation process.

2.4 Time courses and steady-state experiments

Both the time course and the steady-state experiments were performed using the COPASI (COmplex PAthway Simulator) software (Hoops et al. 2006). Time-course simulations were performed for a total of 4 hours with a time-step of 1 second.

3. RESULTS AND DISCUSSION

3.1 Comparison of structures and kinetic laws

Each kinetic model presented earlier describes some of the main metabolic pathways of the central carbon metabolism of *E. coli*. Figure 1 shows a global view of *E. coli* central carbon metabolism, highlighting the reaction coverage of the different models.

All models were compared with regard to their stoichiometric and kinetic structure. Concerning the stoichiometric analysis, all kinetic models were compared against the genome-scale model *i*AF1260. Table 2 shows a summary of all stoichiometric differences identified in all dynamic models when compared with the *i*AF1260. The Khodayari model is the one with the most accurate stoichiometry, since it was constructed based on the *i*AF1260 model, using ensemble modelling (Khodayari et al. 2014). Regarding the Chassagnole, Kadir and Peskov models, some discrepancies were found, for example in the identification of some reactants and products in certain reactions.

The models were then compared regarding the structure of the kinetic equations. The Khodayari model was excluded from this comparison since it is defined in terms of elementary reaction steps. Table 3 presents a summary of all kinetic formats described in the three dynamic models.

Both the Peskov and Kadir models were constructed based on the Chassagnole model, therefore sharing kinetics mechanisms with the latter, although some inconsistencies were found. For instance, the units of parameters and metabolite concentrations are not consistent in the Kadir model and there is also a number of discrepancies between the equations in the SBML file and those described in the model, such as for the isocitrate lyase, and malate and citrate synthase reactions (Kadir et al. 2010).

Finally, another difference was found in the definition of the metabolic cofactors and currency metabolites (e.g ATP, ADP; NADH, CO2, etc.) (Table 4). The Khodayari model explicitly accounts for cofactors in the reaction stoichiometry, whereas the Chassagnole and Kadir models describe them as parameters. The Peskov model treats different cofactors in different ways. It should be emphasized that the cofactors in the Chassagnole model have time-varying properties, given by polynomial equations obtained from fitting experimental data.

3.2 Time course and steady-state experiments

As referred before, the time course experiments have the duration of 4 hours to ensure convergence to a steady state.

Table 2 - Summary of structural and stoichiometric differences identified in the Chassagnole, Kadir, Peskov and Khodayari dynamic models when compared against the *i*AF1260 constraint-based model.

Structural and Stoichiometric differences	Chassagnole	Peskov	Kadir	Khodayari
Missing ADPglucose	GLGC	-	-	-
Missing H^+	GLGC, PFK, GAPD, PYK, PPC , G6PDH2r, PGL	PFK, GAPD, PYK, PPS, PPC, G6PDH2r, PGL, CS, MDH	PFK, PYK, PPC, MDH	GLGC, PFK, GAPD, PYK, PPC , G6PDH2r, PGL
Missing glycogen	G3PD2	-	-	GLCS1
Different reversibility	ENO, PPC, DDPA	FBP, ENO, PPS, PPC, PGL, CS, ACONTa, ACONTb, FUM, MALS	PPC, CS, ACONTa, ACONTb, FUM, MALS	ENO, PPC, DDPA
Missing H_2O	ENO, PPC, DDPA	FBP, ENO, PPS, PPC, PGL, CS, ACONTa, ACONTb, FUM, MALS	PPC, CS, ACONTa, ACONTb, FUM, MALS	ENO, PPC, DDPA
Merged GAP/DHAP pool	-	-	FBA, GAPD, TKT1, TKT2, TALA, AKGDH, SUCOAS	-
Missing Pi	GAPD, PPC, DDPA	-	-	
Reversed direction				
Missing CO_2	PGM, PPC, GND	PGM, PPCK, PPC , ME1, ME2, GND, PDH, ICDHyr, AKGDH	PPC, GND, PDH, ICDHyr, AKGDH, SUCOAS	PGM, PPC, GND
Missing OAA	PPC	-	-	-
Bypasses 6pgl	G6PDH2r, PGL		G6PDH2r, PGL	G6PDH2r, PGL
Divided reaction		TKT1, TKT2, TALA	-	-
Missing CoA	PDH	-		
Missing AcCoA	PDH			
Bypasses acon_C and cit	-		CS, ACONTa, ACONTb	
CoA is a parameter (not a compound)			CS, ACONTa, ACONTb	
Bypasses succoa			AKGDH, SUCOAS	
Missing q8 and q8h2			SUCDi	
Bypasses the actp		PTAr, ACKr	-	
Bypasses Htex		-		CYTBD2pp, Htex
Missing 2dda7p	DDPA			-

Table 3 - Kinetic types of all enzymatic reactions described by three of the analysed dynamic models.

Models / Kinetics Type	Chassagnole	Kadir	Peskov
Nonspecific kinetics	GLCptspp	GLCptspp	GLCptspp
Michaelis-Menten	PRPPS; G3PD2	ACS	-
Reversible Michaelis-Menten	PGMT; ENO; PGM; TPI	-	TPI; ENO; PGM; PGL (foward reaction); RPE; RPI; ACONTa; ACONTb; FUM; EDD
Two-substrate Reversible Michaelis-Menten	GAPD; PGK; PPC; G6PDH2r; GND	GAPD; G6PDH2r; PGL; GND	-
Michaelis-Menten with non-competitive inhibition	-	PDH; ACKr; MALS	
Michaelis-Menten with mixed inhibition		ICL	
Reversible Michaelis-Menten with competitive inhibition	PGI	PGI	PGI
Reversible Mass Action	RPE; RPI; TKT1; TKT2; TALA	RPE; RPI; TKT1; TKT2; TALA	PGL (reverse reaction); TKT1; TKT2; TALA; PTAr; ACKr
Hill equation	PDH; DDPA	-	-
Allosteric Regulation	GLGC; PFKa; PYK	PFKa; PYK; ME2	PFKa; PFKb; FBP1; FBP2; PYK; PPC; ME1; ME2
Ordered Uni Bi mechanism	FBA	FBA; PPC	FBA; EDA
Ordered Bi Bi mechanism	-	CS; ACONTa; ACONTb; MDH	CS; ICDHyr; MDH; MDH2
Ordered Ter Ter mechanism		-	SUCOAS
Random Ter Sequential mechanism		PPCK	-
Random Bi Ter mechanism		ICDHyr	PPCK; G6PDH2r; GND
Random mechanism with competitive inhibition		PTAr	-
Random Bi Bi mechanism		-	GAPD; PGK; SUCDi; ICL; MALS
Ordered Uni Uni mechanism		SUCDi; FUM	-
Ping Pong Irreversible mechanism		AKGDH; SUCOAS	AKGDH
Ping Pong Ter Bi Mechanism		-	PDH
Ping Pong Uni Bi Bi Uni Mechanism			PPS

Table 4 – Different assumptions for cofactors assumed in each model analysed.

Models / Cofactors	Khodayari	Chassagnole	Kadir	Peskov
ATP/ADP/AMP	metabolite	parameter	parameter	metabolite
NAD/NADH	metabolite	parameter	parameter	metabolite
NADP/NAPDH				
CO_2/ H_2O	metabolite	-	-	-
CoA	metabolite	-	parameter	metabolite
Pi	metabolite	-	parameter	parameter
H	metabolite	-	parameter	-
q8/ q8h2	metabolite	-	-	metabolite
Mg	-	-	-	parameter
HCO_3	-	-	-	parameter

However, only the first hour of simulation is presented. The time-course profiles of extracellular glucose, fructose-6-phosphate, pyruvate, isocitrate and acetyl-coA are embedded in Figure 1. Figure 2 shows the time-profiles for metabolites representative of each of the pathways covered: 6-phosphogluconate, fructose-1,6- diphosphate, glyoxilate and fumarate.

It can be observed that the time-course profiles are quite different between the models, although they were simulated with the same environmental conditions. We then compared the steady-state flux distributions obtained by the models to understand if they could reach a similar steady-state despite the different transient profiles (Figures 3 and 4). It can be observed that the steady-state flux distributions also differ for the three models.

It is possible to observe that the fluxes obtained using the Peskov model are generally lower than the ones obtained using the Chassagnole model. By inspecting figures 1 and 2, It can also be observed that most metabolites accumulate in a significantly higher level for the Kadir model (except for isocitrate) when compared with the remaining models. In fact, it seems that, for this model, the chosen kinetic laws for some reactions in the TCA cycle are constraining the corresponding metabolic fluxes, inducing the accumulation of metabolites upstream. The opposite occurs with the Peskov model, that seems to have metabolic bottlenecks defined upstream that induce a low accumulation downstream, a fact that can also be deduced by the differences in external glucose dynamics for this model.

3.3 Experimental Validation

Finally, an experimental validation was performed to evaluate the accuracy of the kinetic models in reproducing experimental data under different environmental conditions.

For this analysis the experimental dataset published by Ishii et al (2007) was used (Ishii et al. 2007). The data were downloaded from the KiMoSys database (Costa et al. 2014) .

In this case study, the experiment was carried out in a glucose-limited chemostat culture of *E. coli* K-12 BW25113 and different genetic and environmental perturbations were tested, including 24 single-gene knockouts cultivated at a dilution rate

of 0.2 h^{-1}, and wild-type strains cultivated at different dilution rates (0.1 - 0.7 h^{-1}).

The four different models were used to replicate these experiments by computing the steady-state flux distribution. Wild-type simulations at all 5 different dilution rates were performed. Only three of the 24 single-gene knockouts were selected for simulation (gnd, talA, pyk), since they belong to glycolysis and the pentose phosphate pathways, which are described by all kinetic models.

To perform a more accurate analysis, the error between the experimental fluxes and the ones obtained with the four kinetic models were analysed. Two different metrics were used, a normalized Euclidean distance and the Pearson correlation coefficient. Figures 5 and 6 present the error distribution across all experimental conditions for each model

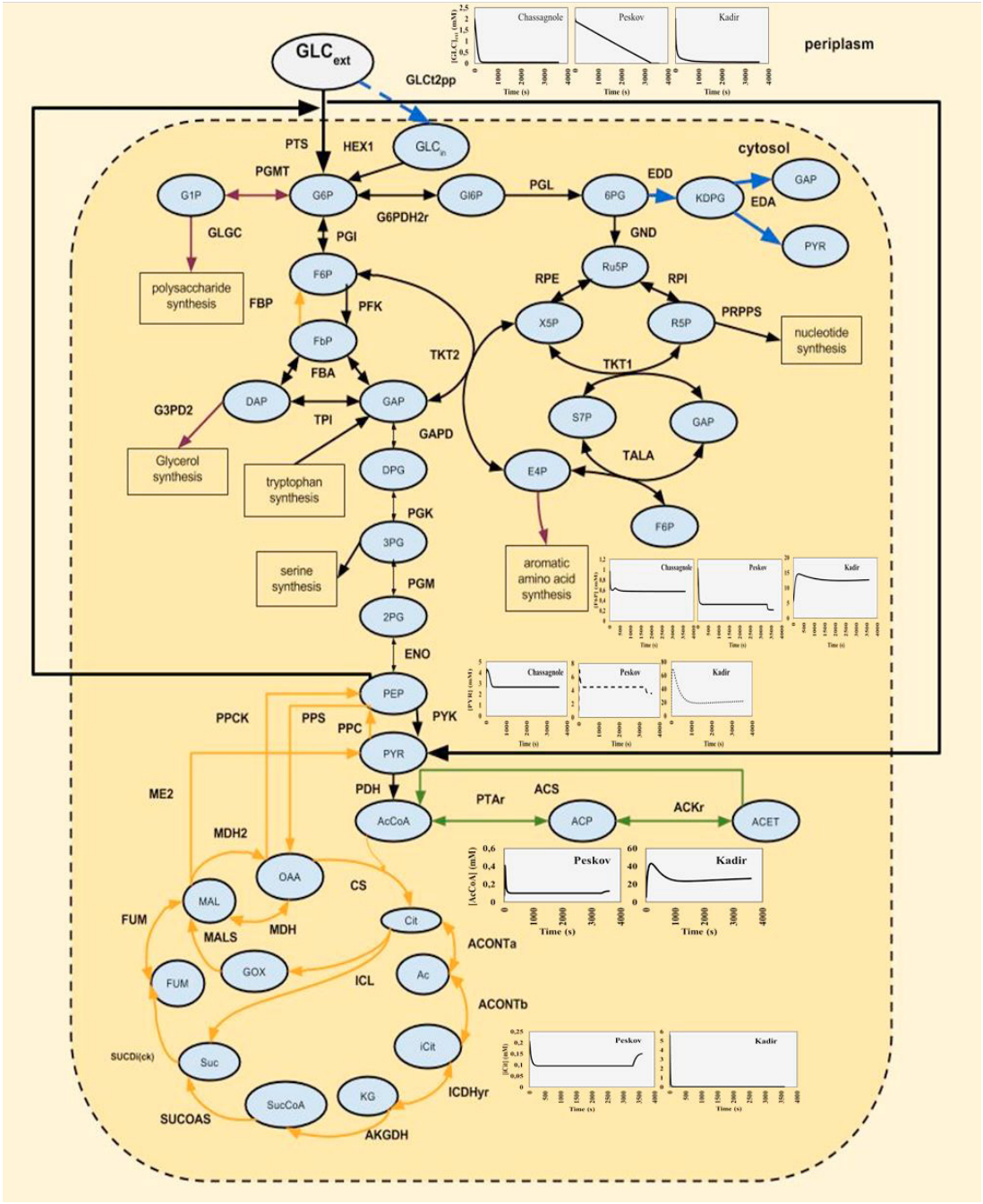

Figure 1 - *Escherichia coli* core central carbon metabolism. The pathways described by three dynamic models, Chassagnole, Peskov and Kadir, are distinguished by different colors. Glycolysis and pentose phosphate pathway, described by the three models, are marked black. Orange represents pathways (TCA cycle and gluconeogenesis) describe by Peskov and Kadir. The Entner–Doudoroff pathway, only described by the Peskov model, is marked blue. Pyruvate metabolism (e.g. acetate formation) is describe by the Kadir model and is represented in green. Pathways marked purple are only described by the Chassagnole model. Note that all the pathways shown in this figure are described by the Khodayari model. The reaction IDs may be found at the BiGG database (*http://bigg.ucsd.edu/*) (Schellenberger et al. 2010)

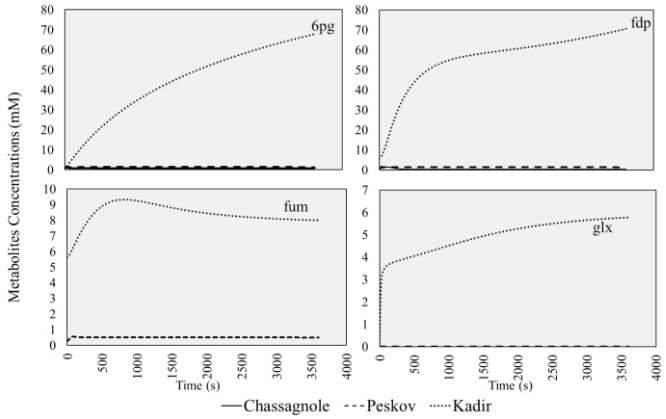

Figure 2 – Time profiles for some metabolites representative of the pathways covered by the models: 6-phosphogluconate, fructose-1,6-diphosphate, glyoxilate and fumarate. For these experiments, a glucose pulse of 2 mM was applied.

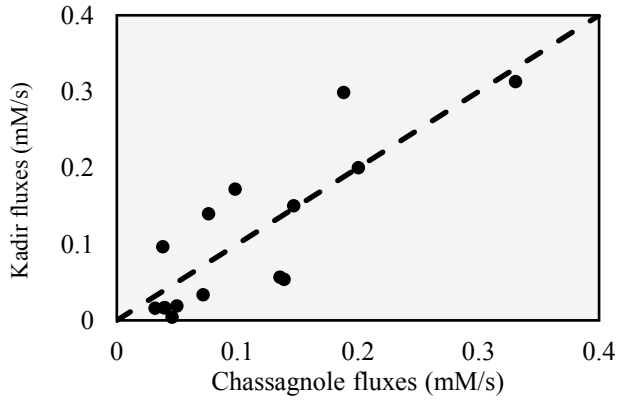

Figure 3 - Reaction fluxes (in steady-state) obtained with the Kadir model compared against to the ones obtained with the Chassagnole model.

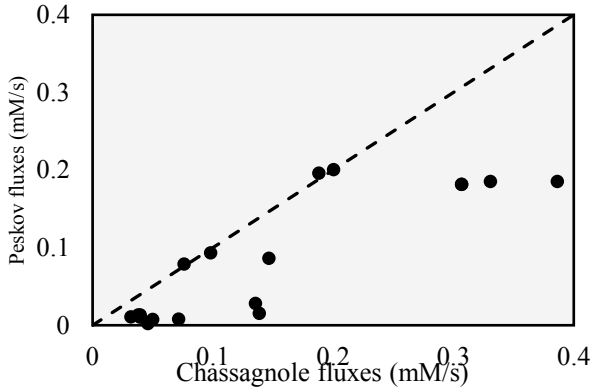

Figure 4 - Reaction fluxes (in steady-state) obtained for the Peskov model compared against to the ones obtained with the Chassagnole model.

It can be observed that the Khodayari model obtained the highest error in terms of Euclidean distance between simulated and experimental fluxes (Fig. 5). This can be explained by the fact that this model was calibrated for a glucose uptake rate of 100 mmol/gDW/h, which is at least one order of magnitude above the experimental values. However, the model performs similarly to the other models when the flux distributions are compared using the Pearson correlation (Fig. 6).

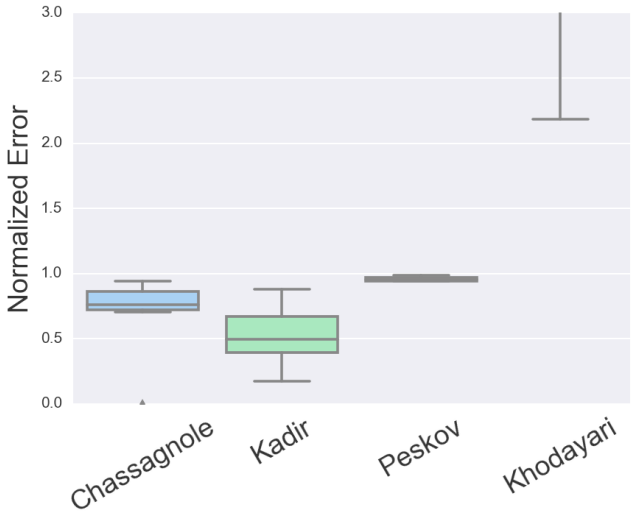

Figure 5 – Distribution of the error between the experimental data and the results obtained with the four kinetic models using the Euclidean distance (please note that the results for the Khodayari model are off the scale, to ensure that the results for the other three models are more clearly visible)

The Kadir model seems to show a higher accuracy with comparison to the other models, showing a smaller Euclidean distance as well as a higher Pearson correlation between simulated and experimental fluxes. The Chassagnole model seems to be the second most accurate model, with an average Pearson correlation above the Peskov and Khodayari models.

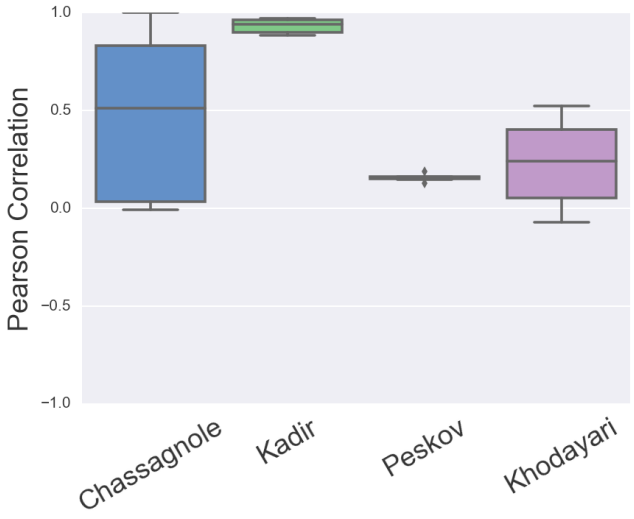

Figure 6 - Distribution of the error between the experimental data and the results obtained with the four kinetic models using the Pearson coefficient.

4. CONCLUSIONS

In this work four dynamic models of the central carbon metabolism of *E. coli* were analysed: Chassagnole (2002), Kadir (2010), Peskov (2012) and Khodayari (2014) regarding their kinetics and stoichiometry, as well as the performance in

predicting the effects of a glucose pulse both in the dynamic behaviour and the reached steady state.

The results obtained in this work demonstrate some differences in both the stoichiometry and kinetic laws regarding the Chassagnole, Kadir and the Peskov models. Also, it proved extremely difficult to perform comparisons both in terms of model structure and simulation outcomes, due to several facts. In the first place, only one of the models (Khodayari, 2014) used standard nomenclature so that a cross comparison of the used entities (metabolites and reactions) could be easily performed. The same was observed for all models regarding the kinetic structure and parameters. The fact that different models made use of different units also hampered any comparison and also complicated the detection of inconsistencies.

The comparison of simulation results performed in this work showed that the models can behave quite differently both in terms of transient profiles and steady-state flux distributions. Comparison with experimental data revealed higher accuracy for one of the models (Kadir 2010). However, more systematic analysis using different experimental datasets is necessary to evaluate the performance of these models under different experimental conditions.

During the course of this work, another kinetic model for *E. coli* has been published (Jahan et al. 2016). It would be interesting to include this model in future comparisons to analyse its performance with regard to the models evaluated herein.

ACKNOWLEDGEMENTS

The authors thank the project “Dynamics”, Ref. ERA-IB-2/0002/2014, funded by national funds through FCT/MCTES. This study was also supported by the Portuguese Foundation for Science and Technology (FCT) under the scope of the strategic funding of UID/BIO/04469/2013 unit and COMPETE 2020 (POCI-01-0145-FEDER-006684).

REFERENCES

Chassagnole, C. et al., 2002. Dynamic modeling of the central carbon metabolism ofEscherichia coli. *Biotechnology and Bioengineering*, 79(1), pp.53–73.

Costa, R.S., Veríssimo, A. & Vinga, S., 2014. KiMoSys : a web-based repository of experimental data for KInetic MOdels of biological SYStems. *BMC Systems Biology*, 8, p.85.

Feist, A.M. et al., 2007. A genome-scale metabolic reconstruction for Escherichia coli K-12 MG1655 that accounts for 1260 ORFs and thermodynamic information. *Molecular systems biology*, 3(121), p.121.

Hoops, S. et al., 2006. COPASI - A COmplex PAthway SImulator. *Bioinformatics*, 22(24), pp.3067–3074.

Ishii, N. et al., 2007. Multiple high-throughput analyses monitor the response of E. coli to perturbations. *Science (New York, NY)*, 316(5824), pp.593–597.

Jahan, N. et al., 2016. Development of an accurate kinetic model for the central carbon metabolism of Escherichia coli. *Microbial Cell Factories*, 15(1), p.112.

Juty, N. et al., 2015. BioModels: Content, features, functionality, and use. *CPT: Pharmacometrics and Systems Pharmacology*, 4(2), pp.55–68.

Kadir, T.A.A. et al., 2010. Modeling and simulation of the main metabolism in Escherichia coli and its several single-gene knockout mutants with experimental verification. *Microbial cell factories*, 9(1), p.88.

Khodayari, A. et al., 2014. A kinetic model of Escherichia coli core metabolism satisfying multiple sets of mutant flux data. *Metabolic engineering*, 25, pp.50–62.

Kuepfer, L., 2014. Stoichiometric modelling of microbial metabolism. *Methods in Molecular Biology*, 1191(1), pp.3–18.

Li, C. et al., 2010. BioModels Database: An enhanced, curated and annotated resource for published quantitative kinetic models. *BMC systems biology*, 4, p.92.

Machado, D. et al., 2012. Exploring the gap between dynamic and constraint-based models of metabolism. *Metabolic engineering*, 14(2), pp.112–9.

Le Novère, N. et al., 2006. BioModels Database: a free, centralized database of curated, published, quantitative kinetic models of biochemical and cellular systems. *Nucleic acids research*, 34(Database issue), pp.D689–91.

Olivier, B.G. & Snoep, J.L., 2004. Web-based kinetic modelling using JWS Online. *Bioinformatics*, 20(13), pp.2143–2144.

Peskov, K., Mogilevskaya, E. & Demin, O., 2012. Kinetic modelling of central carbon metabolism in Escherichia coli. *The FEBS journal*, 279(18), pp.3374–85.

Research Goup of Costas D. Maranas., 2014. Escherichia coli core metabolism. *A kinetic model of Escherichia coli core metabolism*.

Rizzi, M. et al., 1997. In vivo analysis of metabolic dynamics in Saccharomyces cerevisiae: II. Mathematical model. *Biotechnology and Bioengineering*, 55(4), pp.592–608.

Schellenberger, J. et al., 2010. BiGG: a Biochemical Genetic and Genomic knowledgebase of large scale metabolic reconstructions. *BMC bioinformatics*, 11, p.213.

Shmulevich, I., 2011. Computational Systems Biology. *IEEE Life Sciences*, 541, pp.1–1.

Szallasi, Z., 2006. *System Modeling in Cellular Biology* Z. Szallasi, J. Stelling, & V. Periwal, eds., The MIT Press.

Theobald, U. et al., 1997. In vivo analysis of metabolic dynamics inSaccharomyces cerevisiae : I. Experimental observations. *Biotechnology and Bioengineering*, 55(2), pp.305–316.

Toya, Y. et al., 2007. Direct measurement of isotopomer of intracellular metabolites using capillary electrophoresis time-of-flight mass spectrometry for efficient metabolic flux analysis. *Journal of Chromatography A*, 1159(1-2), pp.134–141.

Tran, L.M., Rizk, M.L. & Liao, J.C., 2008. Ensemble modeling of metabolic networks. *Biophysical journal*, 95(12), pp.5606–17.

Vaseghi, S. et al., 1999. In vivo dynamics of the pentose phosphate pathway in Saccharomyces cerevisiae. *Metabolic engineering*, 1(2), pp.128–140.